

Simulation of the Strong-Motion Records from the 2003 Bam Earthquake in Iran Using Stochastic Technique.

By A. Nicknam¹ and S.Yaghmaei² and A.Yazdani³

Iran University of Science and Technology, Tehran, Iran

ABSTRACT

The main objective of this paper is simulating the strong motion records during the destructive 26th December 2003 Bam earthquake located in south-eastern part of Iran. The two widely used stochastically based seismological techniques, point-source and finite-fault source were used for simulating acceleration time histories. These methods provide incorporation of various factors such as source, path and site effects into simple function form and can be easily modified to account for specific situations or improved information about particular aspects for models.

The results of the synthesized ground motions in the form of acceleration time history, elastic response spectra were validated by comparing with those of observed data using model mean bias. The %90 confidence intervals of the means averaged over the whole stations were obtained and assessed using t-student distribution due. The results showed good agreement between simulated and recorded waveforms as well as elastic response spectra confirming satisfactorily validation of selected source-path-site model parameters.

The decay parameter at four stations was estimated to be used in averaged for the region under study. Moreover, the path-dependent quality factor Q , was estimated at five stations as a model parameter for the sites around the region. The sensitivity of PGA and response spectra against the path-averaged frequency-dependent shear wave crustal quality factor Q , was also studied. The results of the two approaches can be used for estimating the probable ground motion acceleration time-histories to be used in hazard analysis of specific sites in the region under study particularly for performance analysis of existing structures. The ability of the two stochastic methods in simulation strong motions was also shown in this study. This study is a part of retrofitting process of historical buildings in Arge-Ban in Bam city.

Keywords: stochastic model, ground motion generation, simulation, point source, finite-fault model, Bam earthquake, response spectra, decay factor κ .

¹ Associate Professor, Department of Civil Engineering University of Science and Technology (IUST),
Email: A-Nicknam@IUST.ac.ir

² PhD Student of IUST

³ PhD Student of IUST

1- INTRODUCTION

Realistic time-histories acceleration should be used in structural analysis to reduce uncertainties in estimating the standard engineering parameters (Hutchings 1994), particularly for non-linear seismic behaviour of structures. So, designers need to know the dynamic characteristics of predicted ground motion consistent with source rupture for a particular site to be able to adequately design an earthquake-resistant structure.

Simulation of earthquake ground motion at the site of interest for given earthquake magnitude scale, focal depth, source physical properties such as source density, slip function, wave propagation from source-to-site and site effects is the main objective of this paper.

Ground motions are estimated by identifying the major regional faults and propagating seismic waves generated at these potential sources to the site of interest.

The two commonly used techniques, finite-fault and point source methods of Beresnev-Atkinson and Boore (Boore and Atkinson, 1987; Beresnev-Atkinson, 1997, 1998a, b) are used for simulation of the destructive 26 December 2003 Bam main shock. In finite-fault technique the finite source is subdivided into a certain number of elements (faults). Each subfault is treated as a point source while the whole source acts as a point source in point-source technique. Both techniques have an omega-squire spectrum.

2-The earthquake Prone Area of Bam, Iran

Iran as one of the world's most earthquake-prone countries has been exposed to many destructive earthquakes in the past long years. The three regions of Zagros, Alborz, and Khorasan are exposed to high seismicity. According to the hypothesis, the movement of African plate toward the Asian plate, pushing the Arabian plateau and southwest of Asian, leads to the creation of faults and rupture on the earth crust in the most parts of Iran. So Iran is one of the world's most earthquake-prone countries which has been exposed to many destructive earthquakes in the past long years particularly in the north (Alborz), south (Zagros), and north-east parts Khorasan.

The Bam region in the south east part of Iran is located in an active seismic zone. There have also been other large earthquakes in the area in the last 40 years (Figure 1), but the city of Bam has not been affected by such destructive earthquake for at least several hundred years. The World Heritage Site citadel, Arg-e-Bam, was constructed largely in the 1700s out of mud bricks and was considerably destroyed by this earthquake.

A destructive earthquake struck the city of Bam in south east part of Iran at 5:26:52 AM (local time) on Friday, December 26, 2003. The U.N. Office for the Coordination of Humanitarian Affairs (OCHA) reported that the Bam earthquake caused the deaths of approximately 43,200 residents and injured approximately 20,000. Some 75,600 people (14,730 house-holds) were displaced, and 25,000 dwellings were razed (EERI, 2004).

The location of the epicenter of this earthquake have been determined by by IIEES (IIEES, 2003) at 29.01N and 58.26E in 10km SW of Bam town that is close to the coordination mentioned by USGS (28.99N, 58.29 E (USGS, 2003)). The Moment Magnitude of 6.6 for this earthquake (M_w) have been measured based on the preliminary evaluations and the focal depth is estimated to be 8km based on S-P evaluation on the records obtained from the main shock (Ashtari and Zare, 2003).

Seismic body wave and preliminary Envisat radar interferometer analysis shows that the main moment release of the earthquake was right-lateral strike-slip motion on a nearly vertical fault oriented roughly north-south (Talebian et al., 2004). An N-S blind reverse fault believed to have been active during the late Quaternary, the Bam fault, passes some 4 km east of downtown of Bam city and just to the west Baravat city (Berberian, 1976). This fault does not appear to have moved significantly at the surface

trace, but a deeper portion may have slipped during the 2003 earthquake (Talebian et al., 2004). However, earthquake causative fault based on Geometric analysis and using Aster images is supposed to be the north piece of Bam fault (Fu et al., 2004).

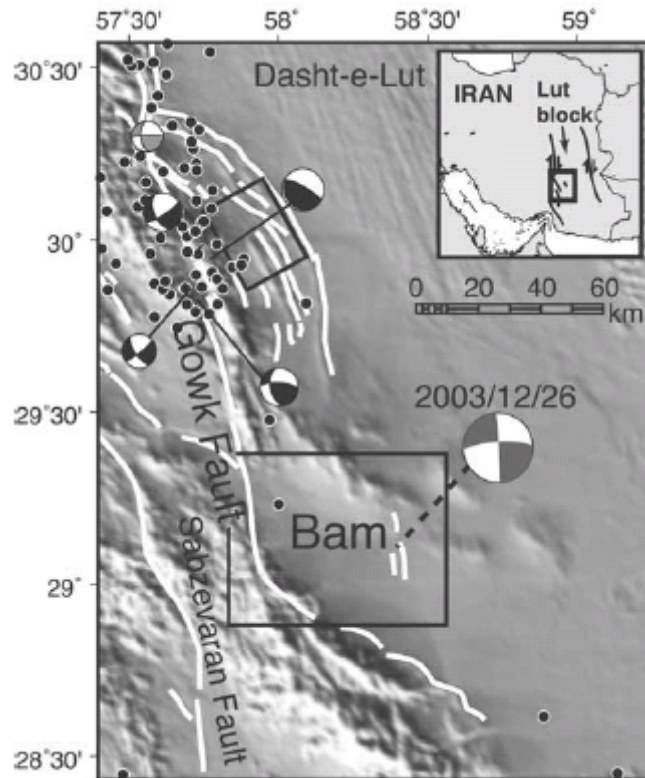


Figure1: Region around Bam with shaded relief (GTOPO30) with light from azimuth 225[Fielding et al. 2005]

3- Stochastic Simulation Method

During the past decades, much effort has been given in reliable simulation of strong ground motion that include theoretical or semi-empirical modeling of the parameters affecting the shape, the duration and the frequency content of strong motion records.

This method is based on the stochastic point source model, which stems out from the work of Hanks and McGuire (1981) who indicated that the observed high frequency ground motion can be represented by windowed and filtered white noise, with the average spectral content determined by a simple description of the source. The stochastic ground-motion modelling technique, also known as the band limited white-noise method, was first described by Boore (1983). Ever since, many researchers have applied the method to simulate ground motion from point sources (e.g., Boore and Atkinson, 1987; Toro and McGuire, 1987; Atkinson and Boore, 1995).

Even though the success of the point-source model has been pointed out repeatedly, it is also well known that it often breaks down, especially near the sources of large earthquakes (Beresnev and Atkinson, 1997, 1998a). Recently, Beresnev and Atkinson (1997) proposed a technique that overcomes the limitation posed by the hypothesis of a point source. Their technique is based on the original idea of Hartzell (1978) to model large events by the summation of smaller ones. In Beresnev and Atkinson (1997) the high-frequency seismic field near the epicentre of a large earthquake is modelled by subdividing the fault plane into a certain number of sub-elements and summing their contributions, with appropriate time delays, at the observation point.

3-1- Stochastic Point source model

The horizontal component of a desired acceleration amplitude spectrum $a(M, R, f)$, defined by a source and a propagation model, is a function of moment magnitude (M) and distance (R):

$$a(M, R, f) = C \times S(M, f) \times D(R, f) \times P(f) \times A(f) \quad (1)$$

Where C is a scale factor, $S(M, f)$ is a source function, $D(R, f)$ is a seismic attenuation function filter, $P(f)$ is a high-frequency truncation filter and $A(f)$ is site amplification (Atkinson and Boore, 1995).

The scaling factor C is given by

$$C = \frac{\langle R_{\nu\phi} \rangle \times F \times V}{4\pi \times \rho \times \beta^3} \quad (2)$$

Where $\langle R_{\nu\phi} \rangle$ is the radiation pattern averaged over an appropriate range of azimuth and take-off angle, F accounts for free surface effects, V represents the partition of a vector into horizontal components. ρ , β are the crustal density and shear wave velocity respectively.

The seismic attenuation function is represented by:

$$D(R, f) = G(R) \times A_n(f) \quad (3)$$

That

$$A_n(f) = \exp \left[\frac{-\pi \times f \times R}{Q(f) \times \beta} \right] \quad (4)$$

Where $G(R)$ a geometric attenuation function is $A_n(f)$ is the anelastic whole path attenuation factor, and Q is the wave transmission quality factor which is defined by the following expression:

$$Q = Q_0 \left(\frac{f}{f_0} \right)^n \quad (5)$$

Where f_0 is the unity frequency (1 Hz), and Q_0 and n are the regional dependent factor and exponent respectively.

The $p(f)$ filter is the upper crust attenuation factor that is used to model the observation that an acceleration spectral density usually appears to fall off rapidly beyond maximum frequency (Hanks, 1982, Silva and Darragh 1995). In the stochastic simulation method, the band limits are the source corner frequency at a low frequency and the high-frequency truncation filter at a high frequency. We applied $p(f)$ as (Anderson, and Hough, 1984):

$$p(f) = \exp(-\pi \times \kappa \times f) \quad (6)$$

The decay parameter Kappa (κ), represents the effect of an intrinsic attenuation upon the wave field as it propagates through the crust from the source to the receiver.

3-2- Stochastic Finite-Fault Simulation Method

Stochastic Finite-Fault Simulation Method is presented by Beresnev and Atkinson (1997, 1998a, b). All simulations are performed using FORTRAN Code FINSIM (Beresnev and Atkinson, 1998). In the adopted methodology, the fault plane is discretized into a finite number of elements (called subfaults), each of which is treated as a point source, and radiations from all subsources are appropriately lagged in time and summed at the observation site. Time histories from individual subsources are generated through the stochastic technique proposed by Boore (1983), assuming that the Fourier amplitude spectrum of the seismic signal at the station is the product of the source spectrum and a number of filtering functions representing the effects of path, attenuation and site response. The subsource spectrum is modeled by multiplying a ω^{-2} spectrum by the Fourier spectrum of windowed Gaussian noise. The duration of the subfault time window (T_w) is represented as the sum of the source duration (T) and a distance-dependent term (T_d):

$$T_w = T + T_d(R) \quad (7)$$

The Fourier acceleration spectrum, $S(M, f)$ at distance R from the subsource has a ω^{-2} shape:

$$S(M, f) = \frac{Cm_0 f^2}{\left[1 + \left(\frac{f}{f_0}\right)^2\right]} \quad (8)$$

The corner frequency (f_0) and seismic moment (m_0) of the subfaults are derived in terms of subfault size (Δl):

$$f_0 = \frac{(yz/\pi)\beta}{\Delta l} \quad (9)$$

$$m_0 = \Delta\sigma\Delta l^3 \quad (10)$$

Where $\Delta\sigma$ is the stress parameter, β is the shear wave velocity, y is the fraction of rupture-propagation velocity to β (assumed equal to 0.8 in the present applications), and z is a parameter physically linked to the maximum rate of slip. The value of z depends on a convention in the definition of the rise time as it is introduced in the exponential functions that describe the ω^{-2} model and for standard conventions $z=1.68$ (Beresnev and Atkinson, 1997, 1998a). Due to the uncertainties involved in the definition of z , its value is allowed to vary through a parameter called s_{fact} , which practically is a “free” parameter during the implementation of the method. FINSIM determines number of subfaults from:

$$N = \frac{M_0}{m_0} = \frac{M_0}{\Delta\sigma\Delta l^3} \quad (11)$$

Where M_0 is the seismic moment of main shock. The lower bound on Δl comes from the requirement that the corner frequency of subfaults lie between the frequency range of interest. FINSIM carries out simulations for frequencies above 0.25 Hz.

4- Model Parameters

During this earthquake, a regional network of 74 strong motion accelerograph stations of the Iranian Strong Motion Network (ISMN), maintained by the Building and Housing Research Center (BHRC), was operating. The stations were equipped with SSA-2 instruments. Among these, 23 stations located within a 1–290 km range of the rupture registered the earthquake with peak acceleration of nearly 1.00–0.01g (see Table 1).

The locations of digital and analog accelerometers and accelerograph station data from the Bam earthquake are shown in Fig. 2 and Table 1 respectively.

The record obtained in Bam station shows the greatest PGA of 0.78g and 0.62g for the east-west horizontal and north-south horizontal components, respectively, and 0.98g for the vertical component (by digital instruments). The preliminary observations on the strong motion record obtained in the

Bam station, as well as the observed damages in the region shows a vertical directivity effect caused by a near-fault effect; therefore we have not selected this station for simulation although it is believed that, the finite-fault techniques can take into account the near-field effects (Hartzel, 1978; Irukura, 1983; Tumarkin 1994; Zeng et al., 1994; Atkinson and Silva, 1997).

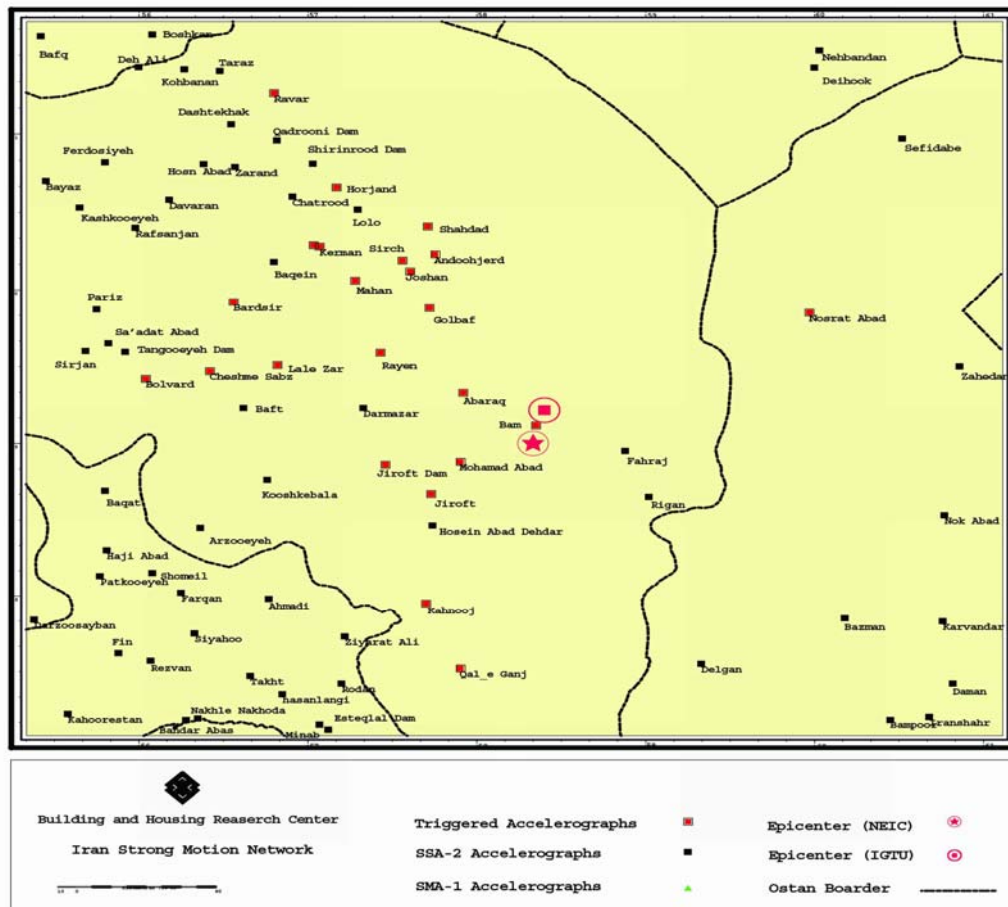


Fig 2. Location of accelerometers near Bam earthquake epicenter

Among the 74 recorded strong motions, 4 stations were chosen so that they have not been affected by near-source as well as directivity effects on the other hand, the source-to-stations distance should be sufficiently far so that the hypothesis requirement of point-source technique for strong motion simulation be applied. The four stations information used in this study are, Mohammad Abad, Abaragh, Golbaft and Jiroft.

The Iran standard soil types (Standard NO. 2800), I and II specified by the average shear wave velocity and the four peak ground amplitudes (PGA) corresponding to each stations are shown in Table 2.

Table 1: Accelerograph station data from the Bam earthquake (BHRC)

NO	Record -No	Station	Coordinates		Geology ^a	Corrected PGA($\frac{cm}{s^2}$)			R ^b (km)
			N	E		L	V	T	
1	3168-2	Bam	29.09	58.35	Clay alluvium fans	778.2	979.9	623.4	10
2	3162	Mohammad -Abad	28.9	57.89	Alluvium fans	115.94	69.17	66.79	49
3	3176-01	Abaragh	29.34	57.94	Evaporate and terrace deposits	116.69	83.81	109.47	52
4	3170	Jiroft	28.67	57.60	Terrace deposits	40.17	30.32	27.56	74
5	3176-02	Rayen	29.59	57.43	Conglomerate and sandstone	14.61	14.67	13.93	107
6	3155	Golbaf	29.88	57.89	Compacted soil	30.29	12.8	27.65	114
7	3166	Kahnootj	27.9	57.7	Silt deposits	10.75	7.76	10.54	133
8	3156	Jooshan	30.12	57.6	Compacted soil	24.88	17.1	36.03	143
9	3164	Andoohjerd	30.13	57.75	Compacted soil	31.82	14.07	33.59	148
10	3161	Sirch	30.20	57.55	Compacted soil	30.28	13.91	29.56	153
11	3159	Mahan	30.6	57.29	Cultivated land	11.99	7.80	13.46	155
12	3180	Lalezar	29.52	56.81	Alluvium fans	12.99	7.6	11.76	158
13	3165	Shahdad	30.41	57.69	Clay and silt deposits	19.77	8.54	13.37	169
14	3163	Qalehganj	27.52	57.87	Alluvium fans	20.28	13.39	22.97	176
15	3160	Nosrat abad	29.86	59.98	Clay and silt deposits	19.13	12.65	23.52	186
16	3175	Kerman	30.28	57.07	Clay deposits	18.87	8.38	30.31	187
17	3157	Kerman	30.29	57.04	Clay deposits	18.45	9.04	24.99	190
18	3169	Cheshmh sabz	29.47	56.42	Young alluvium	22.85	9.11	10.71	194
19	3172	Bardsir	29.92	56.57	Young alluvium	13.58	5.24	10.12	199
20	3174	Horjand	30.67	57.15	Alluvium upper conglomerate and sandstone	6.52	6.14	11.87	218
21	3154	Bolord	29.42	56.05	Decide and deposits	9.68	3.55	10.09	226
22	3187	Zarand	30.81	56.57	Clay and silt deposits	12.10	6.21	12.52	263
23	3173	Ravar	31.26	56.79	Clay and silt deposits	11.99	6.08	12.11	292

^a This column gives the mapped geological unit at the site given by Mirzaei and Farzanegan (1998).

^b Distance is the epicentral distance for all stations. The epicenter was inferred by the strong motion data

5. Estimation of source-path-site parameters

The soil types of Abaragh and Golbaf stations can be classified in soil types I and III respectively (Zare 2004, BHRC). Abaragh and Mohammad Abad Stations, located at the north and south of the event, have about the same epicentral distances, however the geological description (Table 1) for Abaragh and Jiroft is the same and the soil types I can be used for Mohammad Abad and Jiroft stations.

The site amplification factors employed in this paper are given by Boore and Joyner (1997) for the sites characterized by the average shear-wave velocity over the upper 30m (\bar{v}_{30}). The soil types I, III of Iran Standard No.2800, are equivalent to rock and soil types of class D in NEHRP respectively by comparing the average shear wave velocity of the two standards.

Table 2: Most important parameters at selected stations

NO	Station	Soil type (Iran Standard 2800)	Shear wave velocity(cm/se c)	Corrected PGA($\frac{cm}{s^2}$)			kappa
				L	V	T	
ST1	Abaragh	I	$\bar{V}_{30} > 750$	166.69	83.81	109.47	0.02
ST2	Mohammad- Abad	I	$\bar{V}_{30} > 750$	115.94	69.17	66.79	0.05
ST3	Golbaf	III	$175 \leq \bar{V}_{30} < 375$	30.29	12.8	27.65	0.07
ST4	Jiroft	I	$\bar{V}_{30} > 750$	40.17	30.32	27.56	0.09

The material properties described by density ρ , and shear wave velocity β , were estimated to be 2.8 gr/cm^3 and 3.5 km/sec , respectively. For the geometric attenuation, a geometric spreading operator $1/R$ for $R \leq 70 \text{ km}$, $1/R^0$ for $70 < R \leq 130$ and $1/R^{0.5}$ for $R > 130 \text{ km}$ was applied, and the anelastic attenuation was represented by a mean frequency dependent quality factor ($Q(f)$). The selected factors used in this paper are shown in Table 3.

Table 3: Parameters associated with the Q factor (Lam et. al 2000)

No	Region	Q_0	n
1	Quebec(CENA)	755	0.5
2	New Brunswick(CENA)	500	0.65
3	South eastern Canada(CENA)	680	0.36
4	California	204	0.56
5	Victoria, Australia	100	0.85

Aki (1967) recognized that assuming similarity in the earthquake source implies that:

$$M_0 f^3 = \text{const} \tan t \quad (12)$$

where the constant can be related to the stress drop ($\Delta\sigma$). Following Brune (1970, 1971), the corner frequency is given by the following equation:

$$f_0 = 4.9 \times 10^6 \times \beta \times \left(\frac{\Delta\sigma}{M_0} \right)^{\frac{1}{3}} \quad (13)$$

Where f_0 is in Hz, β (the shear-wave velocity in the vicinity of the source) in km/s, $\Delta\sigma$ in bars, and M_0 in dyne-cm. The value of stress drop used as an input data in point source modeling was estimated from equation (13) by assuming the corner frequency of this earthquake $f_0 = 0.18 \text{ Hz}$ (Mostafazadeh, 2004) and $M_w = 6.6$ (USGS). Thus we have used the $\Delta\sigma = 105 \text{ bar}$ as a stress drop parameters in point source modelling of Bam earthquake in different station. However, it is believed that the stress drop should be modeled in a dynamic form rather Atkinson suggests a value of 50 bars ends with more accurate results (Beresnev, I. A. and G. M. Atkinson, 1998a).

In general, the distribution of slip is not known for future events. This motivates us to ask the question: How well could the ground motions is synthesized if the slip distribution were not known? To answer this question, we have applied a randomly drawn slip in our simulations for different stations in finite-fault modeling. We assume that the geometry and location of a given seismogenic fault may be defined with reasonable accuracy, at least in principle; thus, we do not vary the location or geometry of the rupture surface.

5-1-Decay parameter determination, kappa

The frequency independent exponential amplitude decay parameter kappa, as a means of estimating the attenuation for entire source-receive path [Anderson and Hough 1984], is determined for selected stations in this study. By paying attention to the fact that, in omega-squire model, the Fourier Amplitude spectrum requires being flat below the corner frequency, any slope in this part of the data should be due to attenuation. For this purpose, after baseline correction of records, the low and high frequencies have been selected separately and a linear fit was made to this slope using least square method in the semi-log domain. Table 2 shows the average values of this parameter for L and T components of the earthquake. All parameters used for simulation in finite-fault modeling are summarized in Table 4.

Table 4. Modeling parameters for finite fault modeling

Parameters	Bam earthquake
Fault Dimension(km)	20×16
Fault Orientation	Strike 175 ⁰ , dip 85 ⁰
Mainshock moment magnitude(M)	6.6
Stress parameter(bar)	50
Subfault dimension(km)	5×5.33
Number of subfaults	12
Rupture velocity	0.8× shear wave velocity
Crustal shear wave velocity(km/sec)	3.5
Crustal density($\frac{g}{cm^3}$)	2.8
Geometric spreading	$\frac{1}{R}$ ($R \leq 70km$), $\frac{1}{R^0}$ ($70 < R \leq 130$), $\frac{1}{R^{0.5}}$ ($R > 130km$)
$Q(f)$	Based on Table 3
Windowing function	Saragoni-Hart
Kappa operator	Based on Table 2

6- Results, Model Validation and Discussion

After determining the source and path model parameters as mentioned above, the Bam earthquake was simulated for 4 stations regarding the site effects by using the aforementioned process. Figures 3-14 show the comparison of estimated and observed accelerograms as well as response spectra. As it can be seen, good agreement between the simulated and observed data confirms the validation of the selected regional parameters as well as the ability of both techniques.

It is worth to mention that, records of the two horizontal components are obtained from orthogonally oriented components, and thus two records are available at each station. Comparison of the simulated with each of which and/or combination of the two components seems to be questionable. There are a number of ways of using the two horizontal components in strong motion procedure [Douglas 2003]. In this research work, these two records were combined into a single measure of shaking by forming the geometric mean of elastic response spectrum for each component [Boore 2006]. The geometric mean is now the most widely used horizontal-component definition in Ground-motion prediction equations. The geometric mean of the spectral values of the x and y components for the period T_i is defined as:

$$S_{a_{GMXY}}(T_i) = \sqrt{S_{a_x}(T_i) \times S_{a_y}(T_i)} \quad (14)$$

It can be easily demonstrated that, this is equal to the antilog of the arithmetic mean of the logarithms of the accelerations in the two orthogonal directions. Because this is currently the most widely used definition of the horizontal component of motion, it was adopted as the reference definition for calculating ratios in this study.

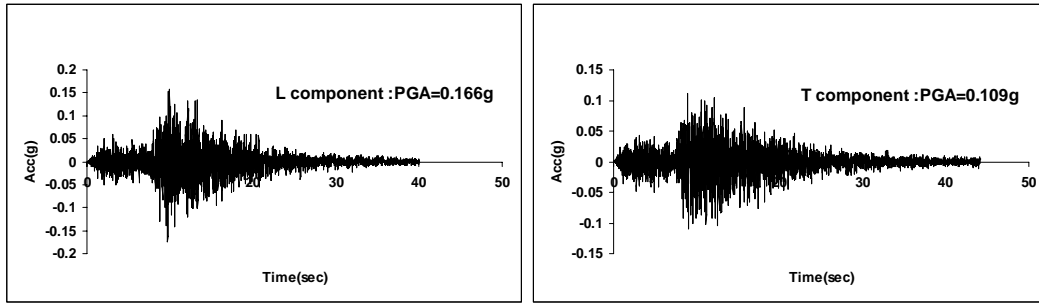


Figure 3.Observed horizontal acceleration (L and T components) time history in St1

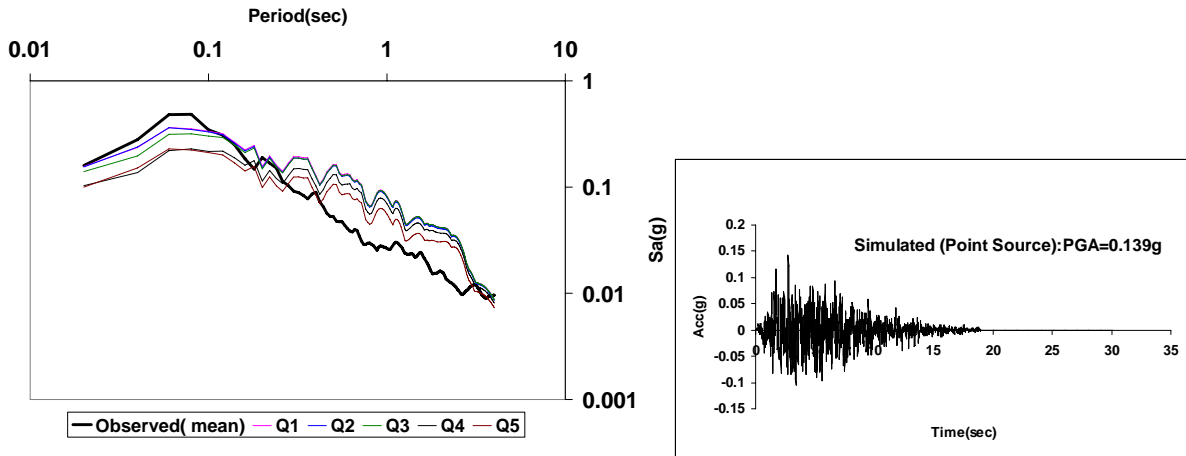


Figure 4.Simulated and observed 5 %-damped pseudo-acceleration response spectra and simulated acceleration time history (Q4) for St1 in Point source

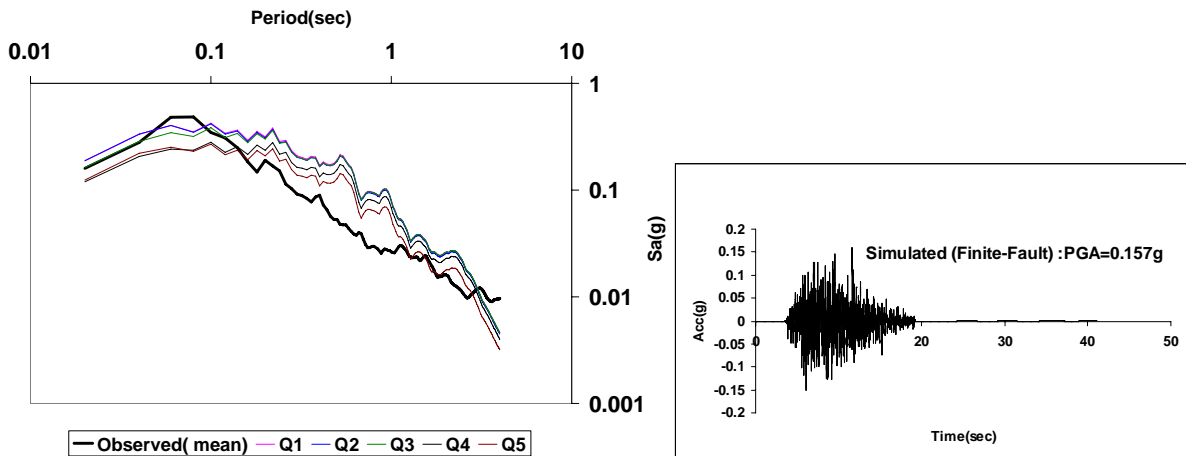


Figure 5.Simulated and observed 5 %-damped pseudo-acceleration response spectra and simulated acceleration time history (Q4) for St1 in Finite-Fault modeling

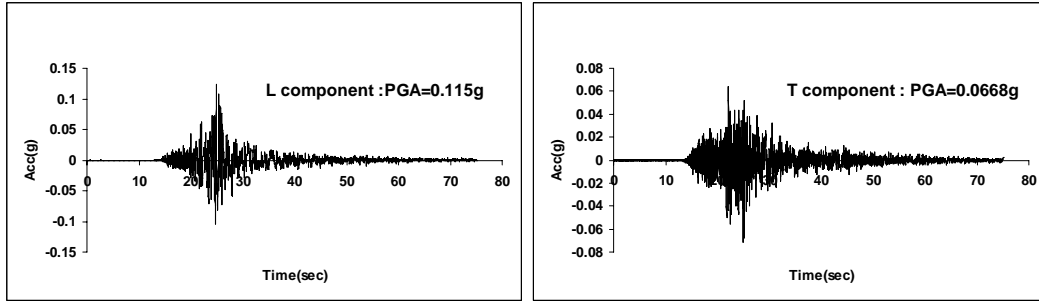


Figure 6.Observed horizontal acceleration (L and T components) time history in St2

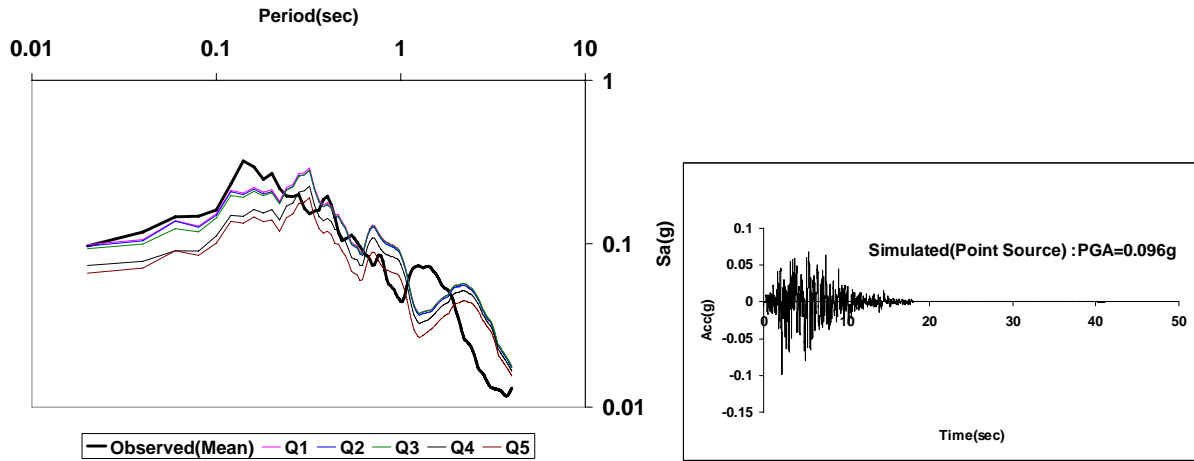


Figure 7.Simulated and observed 5 %-damped pseudo-acceleration response spectra and simulated acceleration time history (Q4) for St2 in Point source

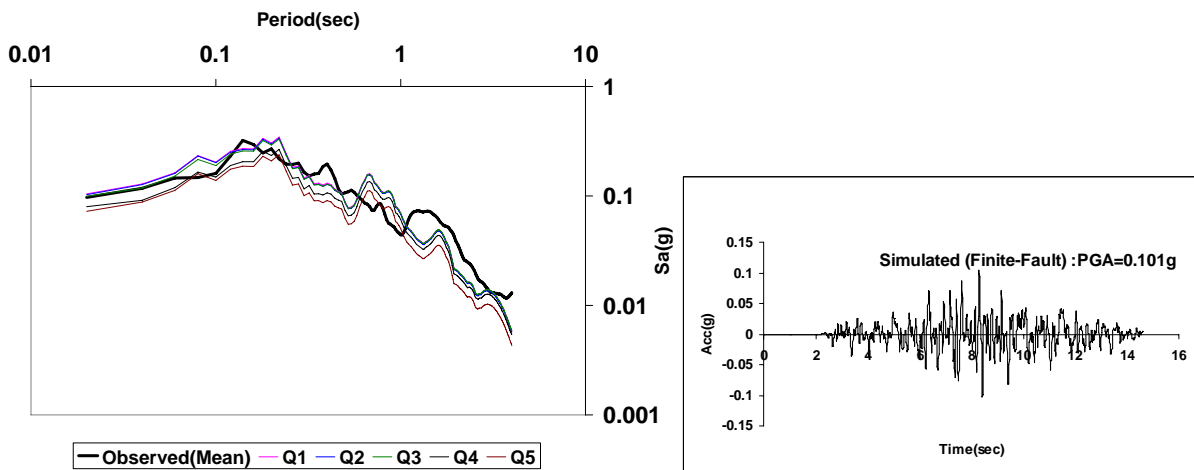


Figure 8.Simulated and observed 5 %-damped pseudo-acceleration response spectra and simulated acceleration time history (Q4) for St2 in Finite-Fault modeling

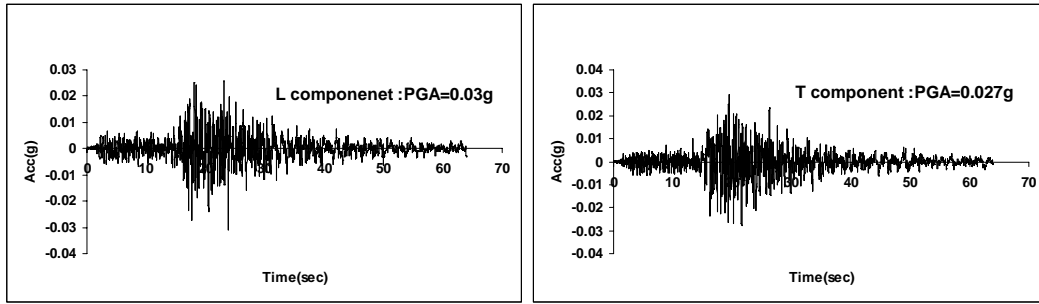


Figure 9.Observed horizontal acceleration (L and T components) time history in St3

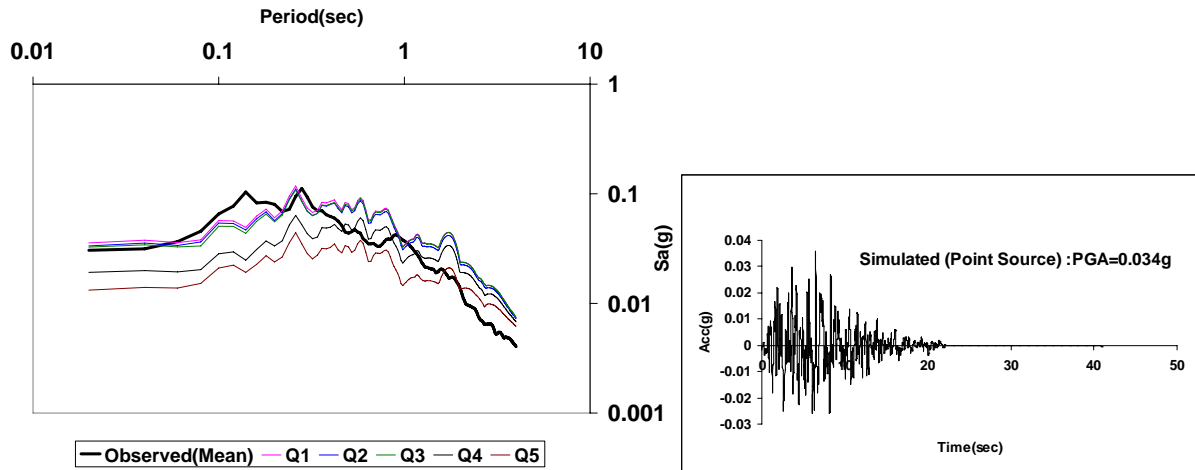


Figure 10. Comparison %5 acceleration response spectra of the observed and simulated time-history for ST3 in point-source

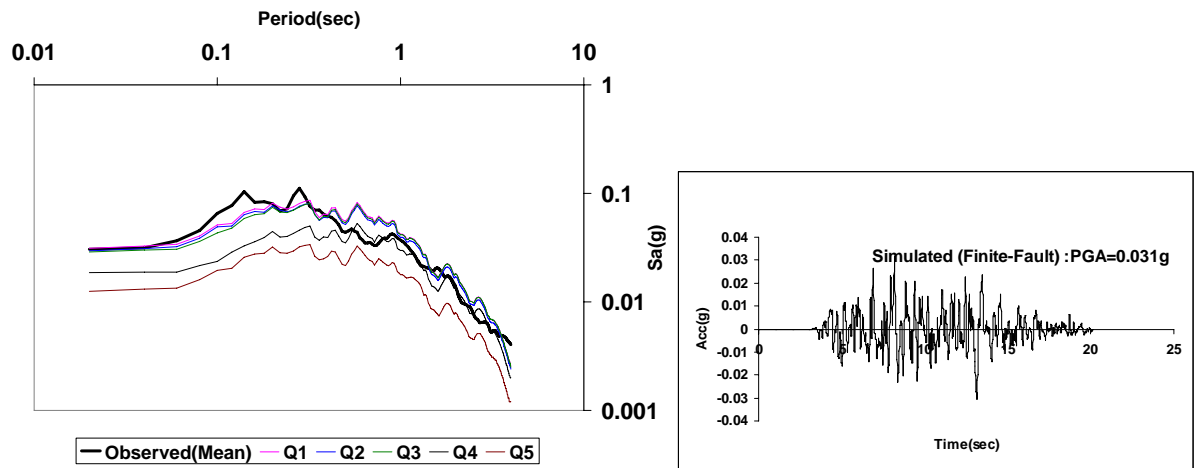


Figure 11.Simulated and observed 5 %-damped pseudo-acceleration response spectra and simulated acceleration time history for St3 in Finite-Fault modeling

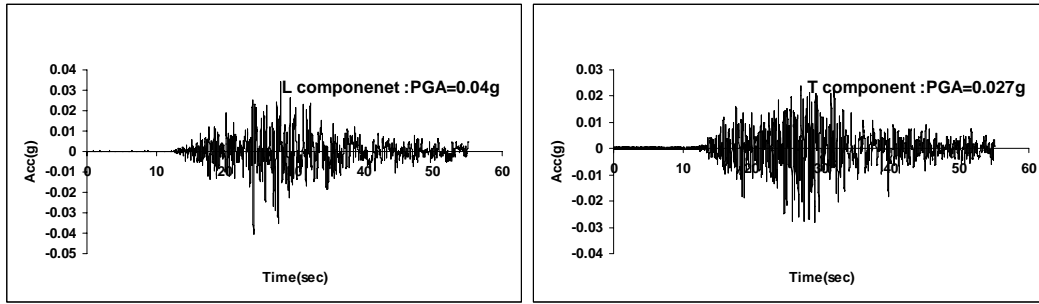


Figure 12. Observed horizontal acceleration (L and T components) time history in ST3

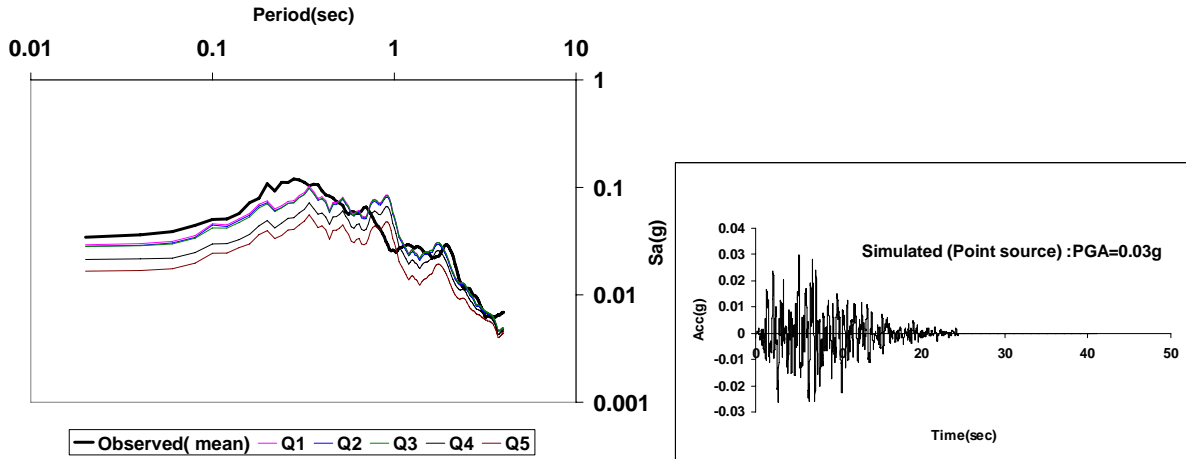


Figure 13. Simulated and observed 5 %-damped pseudo-acceleration response spectra and simulated acceleration time history (Q4) for St3 in Point source

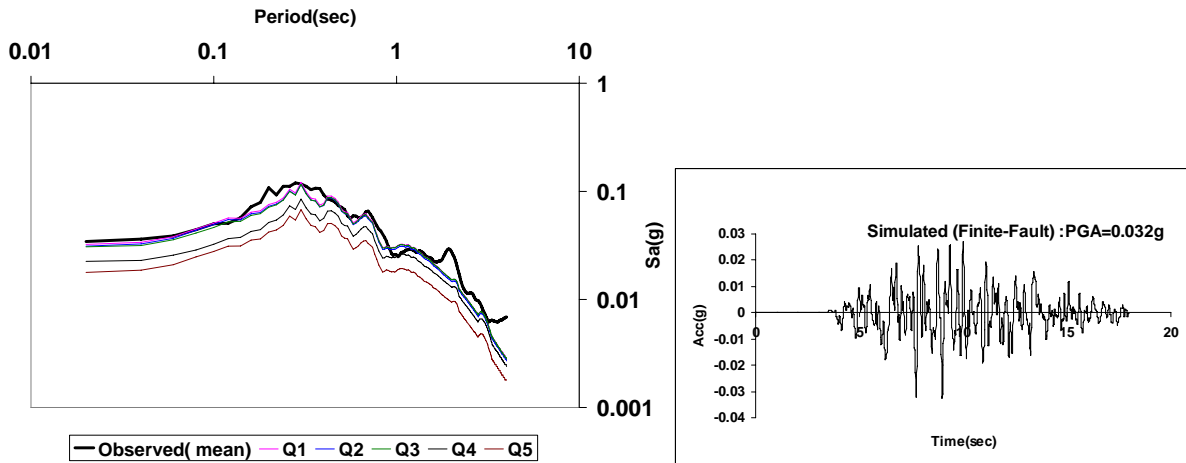


Figure 14. Simulated and observed 5 %-damped pseudo-acceleration response spectra and simulated acceleration time history (Q4) for St3 in Finite-Fault modeling

In order to assess the validation of the simulated earthquakes against recorded horizontal acceleration time histories, the Model Bias was used. MB is defined as the ratio of the observed to the simulated spectrum at each individual station, averaged over all stations (Atkinson and Boore, 1998; Atkinson and Silva, 2000; Beresnev and Atkinson, 2002). In this research work, the elastic acceleration response spectra of simulated and observed acceleration time histories of The Bam earthquake at the selected stations (where the main shock were recorded by digital accelerographs), were compared and the MB of the results if the elastic response spectra were estimated at each individual frequency. The frequency range of this study is 0.25Hz to 50Hz. Due to limited data, the t-student distribution with three degree of freedom ($df=3$) was used for calculating 90% confidence interval of the mean value (the df is equal to the sample size minus 1). Figs (15) and (16) show the results of such estimation with

dashed lines. The obtained results are quite comparable with those of Beresnev et al (Beresnev and Atkinson, 1998a, b) confirming that the finite-fault radiation technique has the potentiality of providing accurate prediction of the mean spectral content of earthquake acceleration time histories. It can be seen from Figs 15 and 16, that, the mean spectral content of amplitude ratios (i.e. the ratios of observed to simulated spectral amplitudes) are not significantly far from unity at the 90% confidence interval.

The results of finite-fault were shown to be more accurate than those of point-source technique, however, the results in some frequencies are deviated from unity (frequencies domain 0.9 to 1.35 Hz in point source model), which could be due to the uncertainties of the selected source information as well as source to site model parameters.

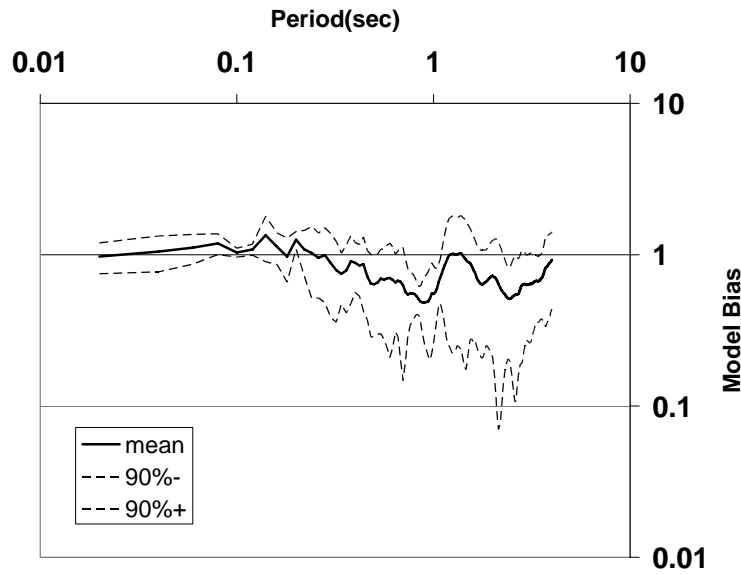


Figure 15. Model bias showing the ratio of observed spectrum, averaged over 4 stations in Point source model

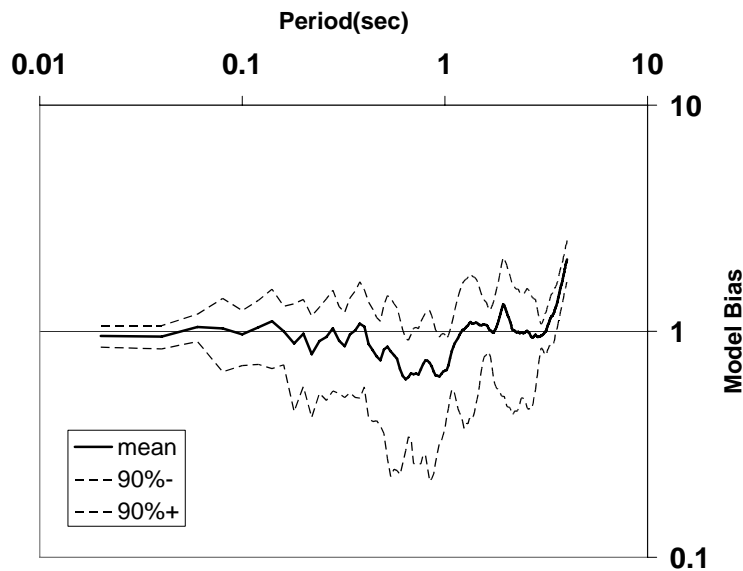


Figure 16. Model bias showing the ratio of observed spectrum, averaged over 4 stations in Finite-Fault model

The path-averaged frequency-dependent shear wave crustal quality factor Q , which is a regional parameter has been used in several studies with different coefficients (Lam 2005, et al). Five different quality factors Q_1 , Q_2 , Q_3 , Q_4 , and Q_5 as shown in Table(3) have been used in this study and the corresponding simulated response spectra were obtained for each station. As it can be seen, the results of Q_1 , Q_2 and Q_3 are approximately close to each other (with quite close for Q_1 and Q_2) and similar to the observed records while those of Q_4 and Q_5 are away from each other and below the response spectra for recorded time histories at all stations using the two techniques (Figs 4-14).

8- Conclusions

We estimated the strong motion during the destructive 26th December 2003 Bam earthquake located in south-eastern part of Iran. The simulated time-series were compared with those of the recorded. The following conclusions could be derived from limited number of the synthesized strong motions.

The stochastic point-source/finite faults source techniques were used to simulate the acceleration time history of 2002 Bam Earthquake. Source-path-site model parameters were first validated against their ability to reproduce the PGA and elastic response spectra at free-field four strong motion stations located at 49,52,74,114 kilometers far from epicenter. The results were successful in agreement with the recorded data (90% confidence level for means averaged over the four stations).

-The results of this study confirm that, the hypothesis made in the simulation process such as constant stress drop in both models, density parameter (ρ) based on the shear wave velocity (β) and using Joyner's proposed relation (Boore and Joyner,1997) would ends with successful and adequately accurate results.

- Each of the path-averaged frequency-dependent quality factors Q_1 , Q_2 , or Q_3 can be used as an appropriate model parameter for the region.

- The proposed decay parameter kappa, can be reliably used as a regional model parameter.

- The selected/estimated source-site model parameters of this study can be used for estimating the probable strong acceleration time-histories for the region to be used in hazard analysis of specific sites particularly for performance analysis of exiting structures. This study is a part of retrofitting process of historical buildings in Arge-Ban in Bam city.

REFERENCES

- Anderson, J. and S. Hough (1984) "A model for the Fourier amplitude spectrum of acceleration at high frequency", Bull. Seism. Soc. Am. 74, 1969-1993.
- Atkinson, G. M. and D. M. Boore (1995)" Ground – Motion Relations for Eastern North America", Bull. Seism. Soc. Am. 85, 17 – 30.
- Atkinson, G. M. and D. M. Boore(1998)" Evaluation of models for earthquake source spectra in eastern North America", Bull. Seism. Soc. Am. 88, 917-934.
- Atkinson, G. M. and W. Silva (1997)" An empirical study o earthquake source spectra for California earthquakes", Bull. Seism. Soc. Am. 87, 97 –113.
- Atkinson, G. M. and W. Silva (2000)" Stochastic modeling of California earthquakes", Bull. Seism. Soc. Am. 90, 255 –274.
- Askari, F., Azadi, A., Davoodi, M, Ghayamghamian, M.R., Haghshenas, E., Hamzelo, H., Jafari, M.K., Kamalian, M., Keshavarz, M., Ravanfar, A., Shafiee, A., and Sohrabi-Bidar, A. (2004), "Preliminary Seismic Microzonation of Bam ", JSEE, Special Issue on Bam Earthquake, 69-79.
- Berberian, M. (1976) "Contribution to the seismotectonics of Iran, part II., Materials for the study of the seismotectonics of Iran", Rep. 39, Geol. Surv. of Iran, Tehran.

- Beyer, K., and J. J. Bommer, (2006), "Relationships between Median Values and between Aleatory Variabilities for Different Definitions of the Horizontal Component of Motion", *Bull. Seism. Soc. Am.* 96(4), 1 – 11.
- Beresnev, I. A. and G. M. Atkinson (1997), "Modeling Finite-Fault Radiation from the ω Spectrum", *Bull. Seism. Soc. Am.* 87, 67 – 84.
- Beresnev, I. A. and G. M. Atkinson (1998a), "FINSIM – a FORTRAN Program for Simulating Stochastic Acceleration Time Histories from Finite Faults", *Seism. Res. Let.* 69, 27 – 32.
- Beresnev, I. A. and G. M. Atkinson (1998b), "Stochastic Finite-Fault Modeling of Ground Motion from 1994 Northridge Acceleration, California, earthquake. I- validation on Rock Sites", *Bull. Seism. Soc. Am.* 88, 1392 – 1401.
- Beresnev, I. A. and G. M. Atkinson (1999), "Generic Finite-Fault Model for Ground-Motion Prediction in Eastern North America", *Bull. Seism. Soc. Am.* 89, 608 – 625.
- Beresnev, I. A. and G. M. Atkinson (2002), "Source Parameters of Earthquakes in Eastern and Western North America Based on Finite-Fault Modeling", *Bull. Seism. Soc. Am.* 92, 695 – 710.
- Boore, D. M. (1983), "Stochastic Simulation of High-Frequency Ground Motions Based on Seismological Models of the Radiated Spectra", *Bull. Seism. Soc. Am.* 73, 1865 – 1894.
- Boore, D. M. and G. M. Atkinson (1987), "Stochastic Prediction of Ground Motion and Spectral Response Parameters at Hard-Rock Sites in Eastern North America", *Bull. Seism. Soc. Am.* 77, 440 – 467.
- Boore, D. M. and W. B. Joyner (1997), "Site Amplification for Generic Rock Sites", *Bull. Seism. Soc. Am.* 87, 327 – 341.
- Boore, D.M., Lamprey, J.W., and Abrahamson, N.A" Orientation-Independent Measures of Ground Motion", *Bull. Seism. Soc. Am.* V.2.1, 2006 (accepted for publication).
- Boore M., Watson-Lamprey J. and Norman A. Abrahamson (2006) "Orientation-Independent Measures of Ground Motion" *Bulletin of the Seismological Society of America*; v. 96; no. 4A; p. 1502-1511.
- Borchert, R.D. (1994), "Estimates of Site-dependent Response Spectra for Design", *Earthquake Spectra*, 10, 617-653.
- Brune, J. N. (1970) "Tectonic stress and the spectra of seismic shear waves from earthquakes", *J. Geophys. Res.* **75**, 4997–5009.
- Brune J. (1971) "Correction." *Journal of Geophysical Research*; 76: 5002.
- Douglas, J. (2003) "Earthquake ground motion estimation using strong-motion records: a review of equations for the estimation of peak ground acceleration and response spectral ordinates", *Earth-Science Reviews* 61, 43-104.
- EERI Special Earthquake Report (2004) "Preliminary Observations on the Bam, Iran, Earthquake of December 26, 2003".
- Eshghi, S. and Zare, M. (2003) "Bam (SE Iran) earthquake of 26 December 2003, Mw6.5: A Preliminary Reconnaissance Report", *International Institute of Engineering Earthquake and Seismology (IIEES) report*.
- Fielding E.J., M. Talebian, P. A. Rosen, H. Nazari, J. A. Jackson, M. Ghorashi, and R. Walker, "Surface ruptures and building damage of the 2003 Bam, Iran, earthquake mapped by satellite synthetic aperture radar interferometer correlation", *Journal of Geophysical Research*, Vol. 110, B03302, doi:10.1029/2004JB003299, 2005
- International Institute of Engineering Earthquake and Seismology (IIEES) 2003 "Preliminary Report on the Bam Earthquake," web site: http://www.iiees.ac.ir/Bam_Report_English.
- Fu, B., Ninnomiya, Y., Lei, X., Toda, S. & Awata, Y., 2004. Mapping active fault associated with the 2003 Mw 6.6 Bam (SE Iran) earthquake with ASTER 3-D images, *Remote Sensing Environment*, 92, 153– 157.

- Irikura, K. (1983) "Semi-empirical estimation of strong acceleration motion during large earthquake," Bull. Disaster Prevention Res. Ins. Kyoto Univ. 33, 63-104.
- Ghafory-Ashtiany, M. (2004), "Bam Earthquake of 05:26:26 of 26 December 2003", JSEE, Special Issue on Bam Earthquake, 1-9.
- Geological Survey of Iran (1993), Geological Map of Iran, 1:100000 Series, Sheet 7648-Bam.
- Hartzell, S. (1978), "Earthquake Aftershocks as Green's Functions", Geophys. Res. Lett. 5, 1-4.
- Hanks, T. C. and R. K. McGuire (1981), "The Character of High Frequency Strong Ground Motion", Bull. Seism. Soc. Am. 71, 2071-2095.
- Hanks T.C " f_{max} ", Bull. Seism. Soc. Am. 72, 1867 - 1979, 1982.
- Hutchings, L. (1994) "Kinematic Earthquake Models and Synthesized Ground Motion Using Empirical Green's Functions", Bul. Seis. Soc. Am. 84, pp. 1028-1050.
- Kanamori, H. and Anderson, D. L. [1975] "Theoretical basis of some empirical relations in seismology," Bull. Seism. Soc. Am. 65(5), 1073-1095.
- Lam N., J. Wilson and G. Hutchinson "Generation of synthetic earthquake accelerograms using seismological modelling: A Review", Journal of Earthq. Eng., Vol. 4, No.3, 321-354, 2000.
- McCallen, D.B. and L.J. Hutchings (1996) "Ground motion estimation and nonlinear seismic analysis", Lawrence Livermore National Laboratory, Livermore, CA, UCRL-JC-121667. Proceedings: 12th Conference on Analysis and Computation of the American Society of Civil Engineers, Chicago.
- Mirzaeialavijeh, H., and Farzanegan, E., (1998) "Specifications of the Iranian accelerograph Network Stations", Building and Housing Research Center, Publication No. 280.
- Mostafazadeh, M. (2005) "Moment Tensor Solution of 26 December 2004 Bam Earthquake," Geophysical Research Abstracts, Vol. 7, 00667.
- Seed, R.B., Cetin, K.O., Moss, R.E.S., Kammerer, A.M., Wu, J., Pestana, J.M., and Riemer, M.F. (2001) "Recent Advances in Soil Liquefaction Engineering and Seismic Site Response Evaluation", Proceeding Fourth International Conference on Recent Advances in Geotechnical Earthquake Engineering and Soil Dynamics, California, (SPL-2).
- Silva, W.J., and R.Darragh (1995) "Engineering characterization of earthquake strong motion recorded at rock sites," Palo Alto, Calif: Electric Power Research Institute, TR-102261.
- Talebian, M., et al. (2004), "The 2003 Bam (Iran) earthquake: Rupture of a blind strike-slip fault", Geophys. Res. Lett., 31, L11611, doi: 10.1029/2004GL020058.
- Toro, G. and R. McGuire (1987), "An Investigation into Earthquake Ground Motion Characteristics in Eastern North America", Bull. Seism. Soc. Am. 77, 468-489.
- Tumarkin, A. G. and R. J. Archuleta (1994) "Empirical ground motion prediction," Ann. Geofis. 37, 1691-1720.
- Yamanaka, Y., (2003) "Seismological Note" No.145, Earthquake Information Center, Earthquake Research Institute, University of Tokyo.
- Zare, M., (2004) "Strong Ground Motion Data of the 1994-2002 Earthquakes in Iran: A Catalogue of 100 Selected Records with Higher Qualities in the Low Frequencies" JSEE, Vol. 6. No. 2, 1-17.
- Zeng, Y., G. Anderson, and G. Yu (1994) "A composite source model for computing realistic strong motions," Geophys. Res. Lett. 21, 725-728.